SCIENCE CHINA Materials

ARTICLES

mater.scichina.com link.springer.com

Published online 19 June 2015 | doi: 10.1007/s40843-015-0060-3
Sci China Mater 2015, 58: 447–454

Quasi-solid-state dye sensitized solar cells using supramolecular gel electrolyte formed from two-component low molecular mass organogelators

Zhipeng Huo[1†*], Li Tao[1†], Songyuan Dai[1,2*], Jun Zhu[1], Changneng Zhang[1], Shuanghong Chen[1] and Bing Zhang[2]

A novel supramolecular gel electrolyte formed from two-component low molecular mass organogelators was developed and introduced into quasi-solid-state dye sensitized solar cell (QS-DSSC). This supramolecular gel electrolyte system was prepared by using *N,N′*-1,5-pentanediylbis-dodecanamide and 4-(Boc-aminomethyl)pyridine as co-gelator. Furthermore, the morphologies of the two-component supramolecular gel electrolyte and single-component gel electrolyte were observed by the polarized optical light microscopy, and the charge transport property of the two-component supramolecular gel electrolyte and the kinetic processes of the electron transport/recombination were investigated by the intensity-modulated photocurrent spectroscopy/intensity-modulated photovoltage spectroscopy (IMPS/IMVS). The polarized optical microscopy (POM) revealed that the single-component gel electrolyte was formed as the rod-like fibers, whereas the fibers changed to branched structure in the two-component supramolecular gel electrolyte. Moreover, comparing with the single-component gel electrolyte based QS-DSSC, the electron transport is faster and the electron recombination at the TiO_2/electrolyte interface is slower in the two-component supramolecular gel electrolyte based QS-DSSC. Consequently, an efficiency of 7.04% was obtained by the two-component supramolecular gel electrolyte based QS-DSSC, which is higher than that of the single-component gel electrolyte based QS-DSSC (6.59%).

INTRODUTION

Dye sensitized solar cells (DSSCs) have been attracted significant attention over the past twenty years [1], owing to their outstanding cost-effectiveness, simple fabrication process and high conversion efficiency. Photoelectric conversion efficiency of DSSCs based on liquid electrolyte was up to 13% [2,3]. However, some undesirable properties, such as leaking and evaporation of the liquid electrolyte, significantly affect the long-term stability, which is crucial to the application and commercial production of DSSCs [4,5]. In recent years, the quasi-solid-state DSSCs (QS-DSSCs) turn out to be a good candidate to solve these prombles, and low molecular mass organogelators (LMOGs) have been extensively applied in QS-DSSCs due to their unique characteristics of both good solubility upon heating and inducement of smooth gelation of organic solvent at low concentrations [6,7]. So far, almost all of quasi-solid-state electrolytes based on LMOGs applied in DSSCs have been comprised of single-component LMOGs. Even though these QS-DSSCs have shown some promising results, their charge diffusion coefficients still should be improved to maintain a sufficiently large flux of charge transport, which limits the photovoltaic performance [6,8–10]. This triggered our intetrest in exploring a novel functional gel electrolyte system to improve the performance of QS-DSSCs. Supramolecular, which could be assembled by two or more LMOGs under proper conditions, dirven by non-covalent interactions, has attracted our attention because of their excellent properties due to their unique microstructures.

In this study, we designed a novel supramolecular gel electrolyte comprised of two-component LMOGs (*N,N′*-1,5-pentanediylbis-dodecanamide and 4-(Boc-aminomethyl)pyridine), and firstly introduced this kind of supramolecular gel electrolyte into DSSCs. Subsequently, we studied how the self-assembled microstructures of the supramolecular gel electrolytes influence the electrochemical properties and the photovoltaic performances of the devices. It is interesting that the supramolecular gel electrolyte can expedite the charge transport in the gel electrolyte and improve the photovoltaic performances of QS-DSSCs in comparison with the single-component gel electrolyte.

[1] Key Laboratory of Novel Thin Film Solar Cells, Institute of Applied Technology, Hefei Institutes of Physical Science, Chinese Academy of Sciences, Hefei 230031, China
[2] Beijing Key Lab of Novel Thin Film Solar Cells, North China Electric Power University, Beijing 102206, China
[†] These two authors contributed equally to this research.
[*] Corresponding authors (emails: zhipenghuo@163.com (Huo Z); sydai@ncepu.edu.cn (Dai S))

EXPERIMENTAL SECTION

Synthesis of *N,N′*-1,5-pentanediylbis-dodecanamide

N,N′-1,5-pentanediylbis-dodecanamide (gelator 1, Fig. 1) was synthesized as previously reported [11] by reacting the lauroylchloride (32.6 mL, 0.14 mol) with 1,5-diaminopentane (4.1 g, 0.044 mol) in a mixture of $NaHCO_3$ (0.13 mol), water (150 mL) and ether (150 mL). After the reaction, the solvent was removed under vacuum and the product was obtained as white powder used with further recrystallization by ethanol. The product was confirmed by proton nuclear magnetic resonance (^{1}H NMR ($CDCl_3$): 0.88 (6H, t, J = 6.7 Hz), 1.26 (34H, m), 1.53 (4H, m), 1.63 (4H, m), 2.16 (4H, t, J = 7.6 Hz), 3.25 (4H, dt, J = 5.4, 7.0 Hz), 5.62 (2H, brs)), and elemental analysis (For $C_{29}H_{58}N_2O_2$ (gelator 1), calculated: C 74.62; H 12.52; N 6.00; found: C 74.69; H 12.37; N 6.24). 4-(Boc-aminomethyl)pyridine (gelator 2, Fig. 1) was purchased and used without further purification.

Polarized optical light microscopy

For optical microscopic investigations, a piece of the gel was placed onto a glass slide and protected with a cover slip. The sample was heated to 130°C at a rate of 10°C min^{-1} and the micrographs were obtained during cooling between crossed polarizer using a microscope (DM2500P, Leica, Germany) equipped with a hot-stage (LTSE-420, Linkam, UK) and camera (micropubisher 5.0 RTV, Qimaging, Canada) at a rate of 1°C min^{-1}.

Differential scanning calorimetry (DSC)

The gel to solution transition temperature (T_{gel}) of the gel electrolyte was determined by differential scanning calorimeter (DSC-Q2000, TA, USA). Approximately 5–7 mg of each sample was weighed and sealed in an aluminum pan and heated at a rate of 10°C min^{-1} under nitrogen flow from 25 to 130°C for the DSC measurement.

Linear voltammetric measurements

Linear voltammograms were recorded on a electrochemical workstation (Autolab 320, Metrohm, Switzerland) at 25°C in two–electrode mode of DSSC equipped with a 5.0 μm platinum ultramicroelectrode (CHI107, CH Instruments Inc., USA) as the working electrode, a 1 mm radius platinum disk electrode (CHI102, CH Instruments Inc., USA) as the counter electrode and reference electrode [6]. The steady-state current-voltage curves were obtained at a scan rate of 5 mV s^{-1}.

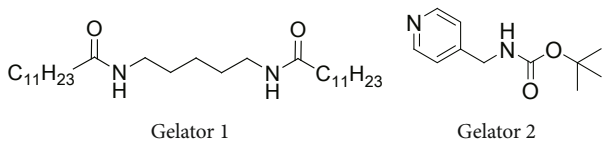

Gelator 1 Gelator 2

Figure 1 Chemical structure of *N,N′*-1,5-pentanediylbis-dodecanamide (gelator 1) and 4-(Boc-aminomethyl)pyridine (gelator 2).

Preparation of the electrolytes

1,2-Methyl-3-propylimidazolium iodide (DMPII) was prepared as reported previously [11]. The liquid electrolyte for DSSCs was composed of 0.1 M iodine (I_2, 99%, Aldrich), 0.1 M anhydrous lithium iodide (LiI: 99%, Aldrich), 0.5 M *N*-methylbenzimidazole (NMBI: 99%, Aldrich), and 1 M DMPII in 3-methoxypropionitrile (MePN: 99%, Fluka). The gel electrolyte A (Gel A) was prepared by adding 4 wt.% (*vs.* liquid electrolyte) gelator 1 into the liquid electrolyte, and the gel electrolyte B (Gel B) was prepared by adding 2 wt.% gelator 1 and 2 wt.% gelator 2 into the liquid electrolyte. The mixtures were heated under stirring until the gelators melted, then the solutions were cooled down to room temperature, and the gel electrolytes A and B were formed. In addition, the chemical structures of gelator 1 and gelator 2 were shown in Fig. 1.

Fabrication of the dye sensitized solar cells

The colloidal TiO_2 mircospheres were prepared by hydrolysis of titanium tetraisopropoxide as described in previous literature [12]. Nanocrystalline electrodes about 9.6 μm thick transparent layer were obtained by screen-printing TiO_2 paste on fluorine doped tin oxide (FTO) glass (TEC-8, LOF, USA). The TiO_2 film was heated in air for 30 min at 450°C. The film was immersed in an ethanol solution of 0.5 mM *cis*-dithiocyanate-*N,N′*-bis-(4-carboxylate-4-tetrabutylammoniumcarboxylate-2,2-bipyridine) ruthenium (II) (N719 dye) for 14 h. The platinized counter electrodes were obtained by spraying H_2PtCl_6 solution to FTO glass followed by heating at 410°C for 20 min. The DSSCs were assembled by sealing the dyed TiO_2 film and the counter electrode with thermal adhesive films (Surlyn1702, Dupont, USA). The liquid electrolyte was injected into the internal space between the two electrodes through the hole on the counter electrode, which were later sealed by a cover glass and thermal adhesive films (Surlyn1702, Dupont, USA). And the gel electrolytes were heated to 130°C under stirring until the gel transform to liquid completely. Then, the electrolyte (hot solution) was injected into the cell and the cell was sealed as the same as the liquid electrolyte. After cooling down to room temperature, a uniform motionless gel layer was formed in the cell.

IMVS/IMPS measurements

The experimental setup for intensity-modulated photocurrent and photovoltage spectroscopy (IMPS and IMVS) measurements have been described elsewhere [13–17]. Intensity–modulated measurements were carried out by an electrochemical workstation (IM6e, Zahner, Germany) with light emitting diodes (λ = 610 nm) driven by a source supply (Export, Zahner, Germany).

Characterization of incidental photon-to-electron conversion efficiency (IPCE)

The photocurrent action spectra were recorded on a QE/IPCE measurement kit consisting of a 300 W xenon lamp (69911, Newport, USA), a 1/4 m monochromator (74125 Oriel Cornerstone 260, Newport, USA), a dual channel power meter (2931-C, Newport, USA) and the calibrated UV silicon photodetector (71675, Newport, USA).

Photovoltaic characterizations

The photovoltaic performance of the DSSCs with an active area of 0.16 cm^2 with black mask were measured by a Keithley 2420 digital source meter (Keithley, USA), and controlled by Test point software under a 450 W xenon lamp (Orial, USA) with a filter (AM 1.5, 100 mW cm^{-2}). The incident light intensity was calibrated with a standard crystalline silicon solar cell before each experiment.

RESULTS AND DISCUSSION

The liquid electrolyte containing 2 wt.% gelator 1 and 2 wt.% gelator 2 as co-gelator can form a mechanically stable two-component supramolecular gel electrolyte (Gel B), and the single-component gel electrolyte (Gel A) was formed with 4 wt.% gelator 1. It is noteworthy that Gel A and Gel B show the remarkable differences in the self-assembly modes which can be clearly seen from the optical micrographs in Fig. 2. The samples were heated to 120°C at a rate of 10°C min^{-1} and cooled to room temperature at a rate of 1°C min^{-1}, then the photograph were obtained. The gelator 1 formed rod-like fibres in Gel A, whereas the co-gelator in Gel B formed branched fibres due to the co-assembly of gelator 1 and gelator 2. In addition, as shown in Fig. 2, the network of Gel A is more compact than that of Gel B. It can be speculated that the charge transport channel in the supramolecular gel network is smoother than that in the single-component gel network.

It is known that, the microscopic 3D network formed by LMOGs has an important influence on the thermodynamic and electrochemical properties of the gel electrolyte [18]. Therefore, the transition temperature (T_{gel}) from gel state to liquid state was measured and used as an important parameter to reflect the intrinsic stability of the gel electrolyte. It is intersting that both gelator 1 and gelator 2 are necessary to access the gel at low gelator contents. Neither gelator 1 nor gelator 2 can form gel electrolyte when the gelator content is below 4 wt.% in a single-component system. Moreover, when we decreased the content of gelator 1 to 2 wt.% and added 2 wt.% gelator 2 into the system to form the two-component supramolecular gel electrolyte, the gelation ability is not significantly weakened. As shown in Fig. 3, the T_{gel} of Gel B is 87°C, which is only slightly lower than the T_{gel} of Gel A (90°C). This phenomenon may result from the less compact gel network of Gel B formed from the two-component co-gelator by co-assembly process. However, both of the T_{gel} values are high enough to ensure the gel state of these two kinds of gel electrolytes at the operating temperature of the devices.

Generally, the increased apparent diffusion coefficients (D_{app}) of redox couple (I_3^-/I^-) in gel electrolyte will result in an improved photocurrent of QS-DSSCs. So increasing the D_{app} is more important for improving the photovoltaic performance of DSSCs. The D_{app} values were calculated from the anodic and cathodic steady-state currents (I_{ss}) using the

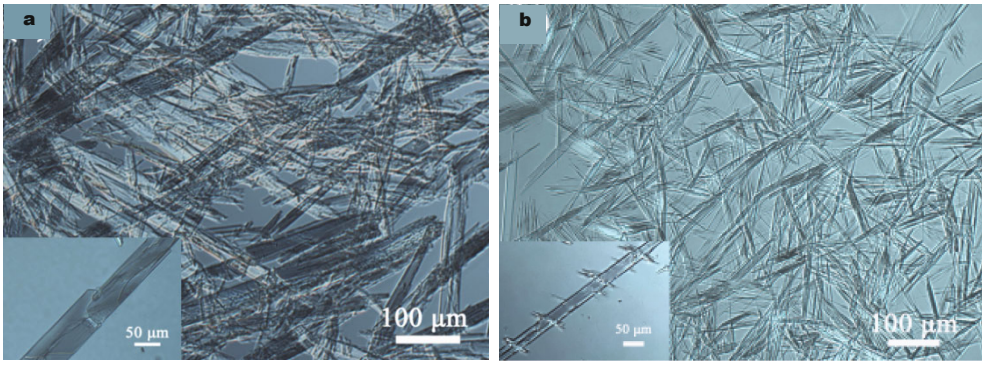

Figure 2 Optical micrographs between crossed polarizer showing the microscopic 3D network structures of (a) Gel A and (b) Gel B. The inset figures show the self-assembled fibers.

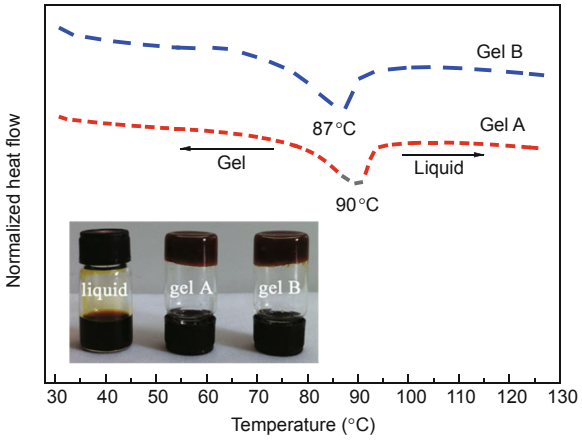

Figure 3 DSC thermograms of Gel A and Gel B.

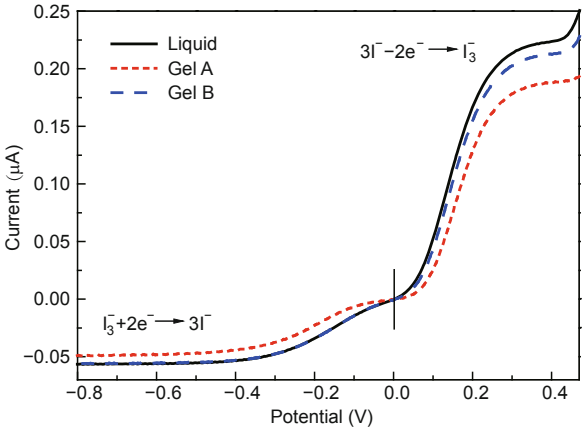

Figure 4 Cyclic voltammograms of liquid electrolyte, gel electrolytes with Pt microelectrode (scan rate = 5 mV s^{-1}).

following equation:

$$I_{ss} = 4nrcFD_{app} \quad (1)$$

where n is the electron number in the electrode reaction, F is the Faraday constant, c is the bulk concentration of electroactive species, D_{app} is the apparent diffusion coefficient, and r is the radius of the Pt ultramicroelectrode. As can be seen in Fig. 4, when the liquid electrolyte is only gelated by gelator 1, the D_{app} values of I^- and I_3^- are both decreased obviously (listed in Table 1). However, when the liquid electrolyte is gelated by the co-gelator containing both gelator 1 and gelator 2, the D_{app} values of I^- and I_3^- are improved and quite close to those of the liquid electrolyte. This favourable result could be attributed to the less compact and more porous gel network of the two-component supramolecular gel electrolyte which provides effective pathways for the transportation of I^- and I_3^-.

In our previous study [18], we found that the amide carbonyl groups of gelators can interact with the lithium ions (Li^+) in the electrolytes. The different gel microstructures and different steric hindrance effects in a single-component gel and supermolecular gel can result in different adsorbing behavior of Li^+ on the TiO_2 film and the electron dynamic processes in the DSSCs. The photoinduced electron density (Q), electron transport time (τ_d) and recombination lifetime (τ_n) for the QS-DSSCs were detected by controlled IMPS/IMVS measurements. The dependence of V_{oc} on ln$Q$ is shown in Fig. 5. As can be seen, in comparison with the liquid DSSC, the TiO_2 conduction band edge of the QS-DSSC based on single-component gelator 1 (Gel A) shifts to more negative potentials. However, in comparison with the QS-DSSC based on Gel A, the TiO_2 conduction band edge of the QS-DSSC based on the two-component co-gelator (Gel B) shifts to more positive potentials and is quite close to the position of TiO_2 conduction band edge in the liquid electrolyte based DSSC. It is accepted that adsorption of Li^+ from the electrolyte to the TiO_2 surface can shift the TiO_2 conduction band edge to more positive po-

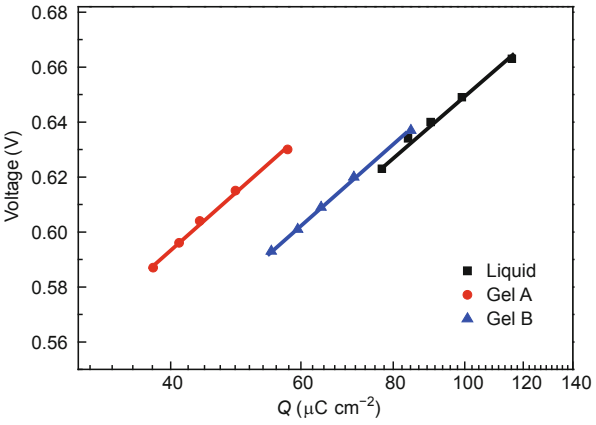

Figure 5 Voltage dependence of the photoinduced electron density in the DSSCs based on different electrolytes.

Table 1 The steady-state limiting currents and apparent diffusion coefficients of iodide and triiodide in different electrolytes

Electrolyte	I_{ss} (I_3^-) (×10^{-7} A)	I_{ss} (I^-) (×10^{-7} A)	D_{app} (I_3^-) (×10^{-6} cm^2 s^{-2})	D_{app} (I^-) (×10^{-6} cm^2 s^{-2})
Liquid	0.57	2.31	1.48	1.63
Gel A	0.47	1.88	1.22	1.33
Gel B	0.55	2.20	1.42	1.55

tentials and increase the charge injection efficiency of the excited state dye [19,20]. The interaction between the gelators and Li^+ in the QS-DSSCs can decrease the adsorption amount of Li^+ on the surface of the mesoporous TiO_2 film and results in the negative shift of TiO_2 conduction band edge in comparison with the liquid electrolyte based DSSC. Furthermore, compared with Gel A, the much smaller fibrils dimension of Gel B decreases the steric hindrance effects on the Li^+ diffusion in the gel network, which facilitates the Li^+ diffusion from the electrolyte to the surface of the mesoporous TiO_2 film, and shifts the TiO_2 conduction band edge to more positive potentials.

The adsorbed Li^+ can intercalate into the TiO_2 lattice and creat extra surface state that strongly influence the kinetic processes of the electron transport/recombination in DSSCs [20,21]. Compared with Gel A, the decreased steric hindrance effect of the supramolecular gel network on the diffusion of Li^+ in Gel B increases the adsorption amount of Li^+ and surface states on the surface of the mesoporous TiO_2 film, which results in much longer electron transport time (τ_d) and electron recombination lifetime (τ_n) [22,23]. τ_d is associated with the electron transport process from the injection sites to the transparent conducting oxide substrate, and τ_n is mostly determined by the rate of recombination between the electrons in the TiO_2 films and I_3^- in the electrolyte. As shown in Fig. 6, at the same J_{sc}, both τ_d and τ_n are decreased in both QS-DSSCs based on Gel A and Gel B in comparison with the liquid electrolyte based DSSC. Furthermore, τ_d and τ_n of the QS-DSSC based on Gel B are much longer than those of the DSSC based on Gel A. This phenomenon can be attributed to the quite different microscopic structures of the gel networks and the changed surface state as mentioned above.

Moreover, the electron collection efficiency (η_{coll}) is determined by the competition between the transport of electrons through the TiO_2 film and the recombination of photoinjected electrons with the redox electrolyte or oxidized dye, which could be evaluated by $\eta_{coll} = 1 - \tau_d/\tau_n$ [24] as shown in Fig. 7. As can be seen in Fig. 7, the order of η_{coll} is Gel A < Gel B < liquid. The η_{coll} as an important factor of IPCE will further influence the short circuit photocurrent density.

Fig. 8 presents curves of IPCE and the *J-V* characteristics at AM 1.5 (100 mW cm^{-2}) and under dark condition for DSSCs based on liquid electrolyte and gel electrolytes. And the photovoltaic performances of short circuit photocurrent density (J_{sc}), open circuit potential (V_{oc}) and energy conversion efficiency (η) are listed in Table 2. As shown in Fig. 8, the dark current of the QS-DSSC based on Gel B is slightly smaller than that of the QS-DSSC based on Gel A, but larger than that of the DSSC based on liquid electrolyte. These results are consistent with the results of the electron recombination lifetime (τ_n) shown in Fig. 6. The TiO_2 conduction band edge of the QS-DSSCs shifted to the negtive

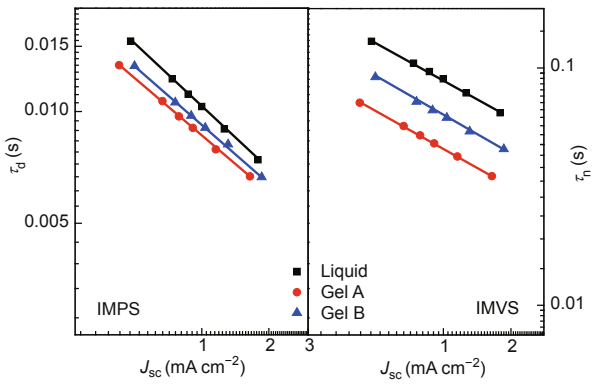

Figure 6 Electron transport time (τ_d) and electron recombination lifetime (τ_n) dependence of J_{sc} in the DSSCs based on liquid and gel electrolytes.

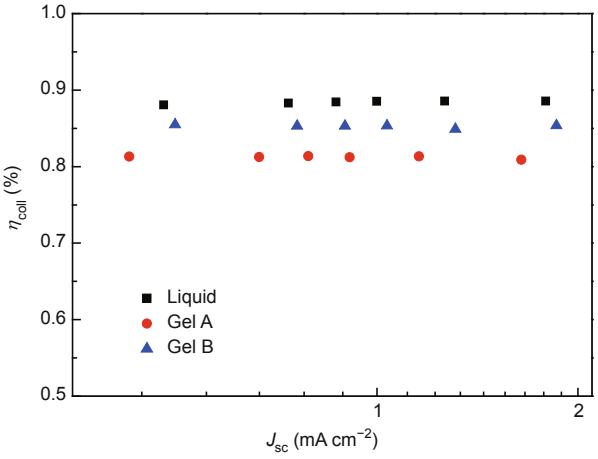

Figure 7 Electron collection efficiency (η_{coll}) dependence of J_{sc} in the DSSCs based on liquid and gel electrolytes.

Table 2 Photovoltaic performance parameters of DSSCs based on liquid and gel electrolytes

Cell	V_{oc} (mV)	J_{sc} (mA cm^{-2})	FF	η (%)
Liquid	701	16.43	0.62	7.11
Gel A	681	15.37	0.63	6.59
Gel B	685	16.38	0.63	7.04

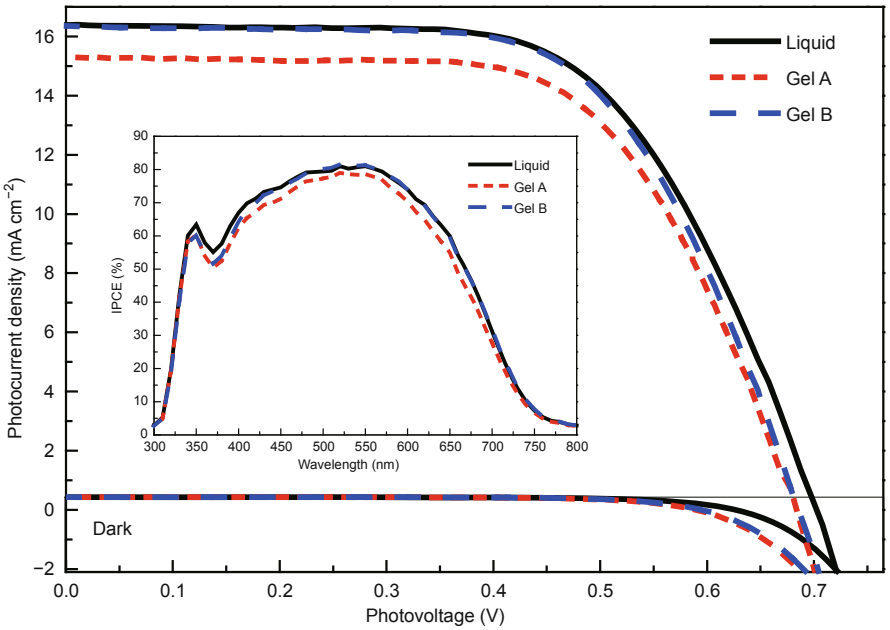

Figure 8 *J-V* curves of different devices at AM 1.5 (100 mW cm^{-2}) and under dark condition. The insert shows the IPCE spectra of the DSSCs based on liquid and gel electrolytes.

position, which would contribute to the V_{oc}. However, on the other hand, the V_{oc} is also influenced by the electron recombination in the TiO_2 photoelectrode/electrolyte interface [14,15]. Therefore, it can be concluded that the lower V_{oc} of QS-DSSCs is mainly caused by the increased electron recombination at the TiO_2/electrolyte interface. Moreover, in comparison with the single-component gel electrolyte, the less compact gel network of the two-component supramolecular gel electrolyte provides more effective pathways for the transportation of I_3^- from TiO_2/electrolyte interface to the Pt counter electrode, which results in a decreased I_3^- concentration at the TiO_2/electrolyte interface. As a result, the reduced electron recombination and increased τ_n was obtained in the QS-DSSCs based on Gel B, which further lead to a increased V_{oc}. According to the previous report [25], the short-circuit photocurrent density (J_{sc}) can be caculated by integrating the product of the incident photon flux density and IPCE used for light absorption by the dye, the J_{sc} is shown as follow:

$$J_{sc} = \int qF(\lambda)[1-r(\lambda)\mathrm{IPCE}(\lambda)\mathrm{D}\lambda \quad (2)$$

where q is the electron charge, $F(\lambda)$ is the incident photon flux density at wavelength λ, and $r(\lambda)$ is the incident light loss before reaching the TiO_2 film in the cell. Also, the IPCE can be caculated by the equation: IPCE = $\eta_{lh}\cdot\eta_{inj}\cdot\eta_{coll}$, where η_{inj} is the electron injection efficiency and η_{lh} is the product of the light-harvesting efficiency of the dye which is considered the same for all of DSSCs in this work. Compared with the DSSC based on Gel A, the IPCE and J_{sc} values of the DSSC based on Gel B are improved obviously, which is attributed to the increased η_{inj} by the positive shift of the TiO_2 conduction band edge shown in Fig. 5 and the increased η_{coll} shown in Fig. 7. It is noteworthy that there is almost no difference in the IPCE and J_{sc} between the DSSCs based on liquid electrolyte and Gel B. Consequently, the supramolecular gel (Gel B) based QS-DSSC shows an impressive efficiency of 7.04%, which is quite close to that of the liquid electrolyte based DSSC (7.11%).

CONCLUSION

In conclusion, for the first time, a novel supramolecular gel electrolyte formed from two-component low molecular mass organogelators was successfully developed for QS-DSSCs. The supramolecular gel network formed from the co-gelator exhibits branched fibrils with much smaller size than those of the single-component gel network, which provides much better charge transport channel. Furthermore, the much smaller fibril size and less compact gel network of the supramolecular gel lead to the higher diffusion of redox species (I^- and I_3^-) compared with the single-component gel, which results in the reduced dark reaction and contributes to the J_{sc} and V_{oc} of the supramolecular gel electrolytes based QS-DSSC. Because of the positive shift of TiO_2 conduction band edge which results from the increased adsorption of Li^+ on the surface of the mesoporous TiO_2 films, the QS-DSSC based on the co-gelator has much

higher η_{inj} than that containing single-component gelator. As a result, the increased η_{inj} and η_{coll} lead to the better IPCE and J_{sc} of the QS-DSSCs based on the co-gelator compared with the single-component gelator. Consequently, the supramolecular gel electrolyte based QS-DSSC exhibits superior photovoltaic performance (η = 7.04%) to the single-component gel electrolyte based QS-DSSC (η = 6.59%), and the efficiency of the QS-DSSC based on the co-gelator can be comparable to that of corresponding liquid elctrolyte based DSSC (η = 7.11%). This result demonstrates an important strategy to obtain QS-DSSCs with high efficiency and good stability using the multi-component supramolecular gel electrolytes.

Received 12 May 2015; accepted 12 June 2015; published online 19 June 2015

1 Oregan B, Grätzel M. A low-cost, high-efficiency solar-cell based on dye-sensitized colloidal TiO_2 films. Nature, 1991, 353: 737–740
2 Nazeeruddin MK, Baranoff E, Grätzel M. Dye-sensitized solar cells: a brief overview. Solar Energy, 2011, 85: 1172–1178
3 Grätzel M. Conversion of sunlight to electric power by nanocrystalline dye-sensitized solar cells. J Photochem Photobiol A, 2004, 168: 235–235
4 Wu JH, Hao S, Lan Z, *et al*. A thermoplastic gel electrolyte for stable quasi-solid-state dye-sensitized solar cells. Adv Funct Mater, 2007, 17: 2645–2652
5 Bisquert J, Cahen D, Hodes G, Ruhle S, Zaban A. Physical chemical principles of photovoltaic conversion with nanoparticulate, mesoporous dye-sensitized solar cells. J Phys Chem B, 2004, 10: 8106–8118
6 Huo ZP, Zhang CN, Fang XQ, *et al*. Low molecular mass organogelator based gel electrolyte gelated by a quaternary ammonium halide salt for quasi-solid-state dye-sensitized solar cells. J Power Sources, 2010, 195: 4384–4390
7 Wang X, Deng R, Kulkarni SA, *et al*. Investigation of the role of anions in hydrotalcite for quasi-solid state dye-sensitized solar cells application. J Mater Chem A, 2013, 1: 4345–4351
8 Kubo W, Kitamura T, Hanabusa K, Wada Y, Yanagida S. Quasi-solid-state dye-sensitized solar cells using room temperature molten salts and a low molecular weight gelator. Chem Commun, 2002, 4: 374–375
9 Suzuki M, Abe T, Hanabusa K. Low-molecular-weight gelators based on N^{α}-acetyl-N^{ε}-dodecyl-L-lysine and their amphiphilic gelation properties. J Colloid Interface Sci, 2010, 341: 69–74
10 Yu QJ, Yu CL, Guo FY, *et al*. A stable and efficient quasi-solid-state dye-sensitized solar cell with a low molecular weight organic gelator. Energy Environ Sci, 2012, 5: 6151–6155
11 Shi CW, Dai SY, Wang KJ, *et al*. Optimization of 1,2-dimethyl-3-propylimidazolium iodide concentration in dye-sensitized solar cells. Acta Phys-Chimi Sinica 2005, 21: 534–538
12 Huang F, Chen D, Zhang XL, Caruso RA, Cheng YB. Dual-function scattering layer of submicrometer-sized mesoporous TiO_2 beads for high-efficiency dye-sensitized solar cells. Adv Funct Mater, 2010, 20: 1301–1305
13 Peter LM, Wijayantha KGU. Electron transport and back reaction in dye sensitised nanocrystalline photovoltaic cells. Electrochim Acta, 2000, 45: 4543–4551
14 Fisher AC, Peter LM, Ponomarev EA, Walker AB, Wijayantha KGU. Intensity dependence of the back reaction and transport of electrons in dye-sensitized nanacrystalline TiO_2 solar cells. J Phys Chem B, 2000, 104: 949–958
15 Dloczik L, Ileperuma O, Lauermann I, *et al*. Dynamic response of dye-sensitized nanocrystalline solar cells: characterization by intensity-modulated photocurrent spectroscopy. J Phys Chem B, 1997, 101: 10281–10289
16 Bisquert J. Theory of the impedance of electron diffusion and recombination in a thin layer. J Phys Chem B, 2002, 106: 325–333
17 Adachi M, Sakamoto M, Jiu J, Ogata Y, Isoda S. Determination of parameters of electron transport in dye-sensitized solar cells using electrochemical impedance spectroscopy. J Phys Chem B, 2006, 110: 13872–13880
18 Tao L, Huo Z, Ding Y, *et al*. Gel electrolyte materials formed from a series of novel low molecular mass organogelators for stable quasi-solid-state dye-sensitized solar cells. J Mater Chem A, 2014, 2: 15921–15930
19 Pelet S, Moser JE, Grätzel M. Cooperative effect of adsorbed cations and iodide on the interception of back electron transfer in the dye sensitization of nanocrystalline TiO_2. J Phys Chem B, 2000, 104: 1791–1795
20 Kopidakis N, Benkstein KD, van de Lagemaat J, Frank AJ. Transport-limited recombination of photocarriers in dye-sensitized nanocrystalline TiO_2 solar cells. J Phys Chem B, 2003, 107: 11307–11315
21 Kopidakis N, Neale NR, Frank AJ. Effect of an adsorbent on recombination and band-edge movement in dye-sensitized TiO_2 solar cells: evidence for surface passivation. J Phys Chem B, 2006, 110: 12485–12489
22 Watson DF, Meyer GJ. Cation effects in nanocrystalline solar cells. Coord Chem Rev, 2004, 248: 1391–1406
23 Kelly CA, Farzad F, Thompson DW, Stipkala JM, Meyer GJ. Cation-controlled interfacial charge injection in sensitized nanocrystalline TiO_2. Langmuir, 1999, 15: 7047–7054
24 Wang YF, Li KN, Liang CL, *et al*. Synthesis of hierarchical SnO_2 octahedra with tailorable size and application in dye-sensitized solar cells with enhanced power conversion efficiency. J Mater Chem, 2012, 22: 21495–21501
25 Tachibana Y, Hara K, Sayama K, Arakawa H. Quantitative analysis of light-harvesting efficiency and electron-transfer yield in ruthenium-dye-sensitized nanocrystalline TiO_2 solar cells. Chem Mater, 2002, 14: 2527–2535

Acknowledgments This work was financially supported by the National Basic Research Program of China (2011CBA00700), External Cooperation Program of Chinese Academy of Sciences (GJHZ1220), the National High Technology Research and Development Program of China (2011AA050510), the National Natural Science Foundation of China (21103197, 21173227, 21403247, 61404142 and 21273242) and the Program of Hefei Center for Physical Science and Technology (2012FXZY006).

Author contributions Huo Z and Tao L wrote this manuscript. Huo Z directly guided and conducted this research including the design, modifying and polishing work related to this manuscript. Tao L performed the main experiments. Dai S supervised the projects and carefully reviewed and modified this manuscript. Zhu J, Zhang C, Chen S and Zhang B provided help in the fabrication of devices and methods of characterization. All authors contributed to the general discussion about this work.

Conflict of interest The authors declare that they have no conflict of interest.

Zhipeng Huo was born in 1982. He is an associate researcher of Hefei Institutes of Physical Science, Chinese Academy of Sciences. He obtained his BSc degree in chemical engineering and technology from Beijing University of Chemical Technology in 2004, and PhD degree in materials physics and chemistry from the Graduate University of Chinese Academy of Sciences in 2009. His current research interests mainly focus on functional electrolytes, electrochemistry for energy conversion and storage devices.

Li Tao was born in 1983. She obtained her PhD degree in materials physics and chemistry from the University of Chinese Academy of Sciences in 2015. Her research interests mainly focus on synthesis, characterization and application of organic compounds, and electrochemical analysis for energy conversion devices.

Songyuan Dai was born in 1967. He is a professor and Dean of the School of Renewable Energy, North China Electric Power University. He obtained his BSc degree in physics from Anhui Normal University in 1987, and MSc and PhD degrees in plasma physics from the Institute of Plasma Physics, Chinese Academy of Sciences in 1991 and 2001. His research interests mainly focus on the next-generation solar cells including dye-sensitized solar cells, quantum dot solar cells, perovskite solar cells, etc.

中文摘要 本文制备了一种由*N*,*N*′-1,5-戊二基双月桂酰胺和4-(Boc-氨基甲基)吡啶作为共胶凝剂的新型超分子凝胶电解质, 并将其应用于准固态染料敏化太阳电池(QS-DSSC)中. 通过偏光显微镜观察超分子凝胶电解质和由*N*,*N*′-1,5-戊二基双月桂酰胺制备的单组份凝胶电解质微观形貌的差异, 并通过调制光电流谱/调制光电压谱(IMPS/IMVS)来研究两种凝胶电解质体系中的电子传输/复合动力学过程. 结果表明, 单组份凝胶电解质中的网络结构是由棒状纤维构成, 而在超分子凝胶电解质中出现分叉纤维结构; 与单组份凝胶电解质组装的QS-DSSC相比, 基于超分子凝胶电解质的QS-DSSC内部电子传输更快且电子在TiO_2/电解质界面处的复合速率更慢. 最终, 基于超分子凝胶电解质的QS-DSSC获得了7.04%的光电转换效率, 高于基于单组份凝胶电解质的QS-DSSC的光电转换效率(6.59%).